An Integrated Robust Strategy for Diagnosing Sensor Faults in Building Chilling Systems

Jin-Bo Wang, Ph.D. **Shengwei Wang, Ph.D.** **John Burnett, Ph.D.**
Member ASHRAE

An integrated robust strategy for the detection, diagnosis, and validation of the soft sensor faults commonly found in building chilling systems is presented. The integrated strategy, which extends the works of Wang and Wang (1999), is based on the universal conservation relationships for mass and energy. Biases in temperature sensors and flow meters are estimated by minimizing the sums of the squares of the mass and energy balance residuals. A robust approach using a genetic algorithm is used to systematically minimize the sums of the squares of the associated heat balance residuals so that the biases are estimated more reliably and accurately. A correlation cancellation method is developed to estimate the cooling water flow meter bias, under conditions in which the cooling water temperature sensor biases exist and are unknown. The correlation cancellation method uses a derived characteristic quantity to estimate the water flow meter bias. Validation tests are performed using a dynamic simulation together with a field case study conducted in an existing building chilling system. Even in unfavorable conditions, the integrated robust strategy can estimate the biases of the chilled and cooling water flow meters and the relative biases of the chilled and cooling water temperature sensors accurately and robustly.

INTRODUCTION

Sensors provide information on the operation of modern building heating, ventilating, and air-conditioning systems. Their reliability is essential to control and monitoring. Faulty sensors that are either completely or partially failed (hard fault or soft fault) provide incorrect information. This can be detrimental to the various schemes that make decisions based on measurements. The unreliability of sensor signals is one of the main obstacles to improving the performance of building control and successfully applying fault detection techniques in automated HVAC commissioning and performance monitoring systems (Kao and Pierce 1983; Usoro et al. 1985; Stylianou and Nikanpour 1996; Lee et al. 1997; Dexter 1999).

Soft sensor faults, such as biases or drifts, are among the typical faults found in building HVAC systems. A conventional engineering method to find and correct the faults is to follow procedures that check and recalibrate the sensors periodically (Pike and Pennycook 1992). This does not satisfy the requirements of modern HVAC systems, which need reliable measurements for continuous online automated schemes. It has also been recognized that it is very difficult, if not impossible, to recalibrate water flow meters after they have been installed into pipelines (Phelan et al. 1996). Therefore, automated online sensor fault detection and diagnosis (FDD) methods that not only indicate when and where a sensor is faulty, but also evaluate the magnitude of the fault, are highly desirable.

Many advanced methods have been proposed for the detection and diagnosis of sensor faults. The model-based method (Patton 1994) is most commonly used in modern FDD schemes. The

Jin-Bo Wang, currently an associate professor in the Faculty of Environmental Science and Engineering, Huazhong University of Science and Technology, Wuhan, is a Ph.D. graduate, **Shengwei Wang** is an associate professor, and **John Burnett** is head and chair professor of the Department of Building Services Engineering, The Hong Kong Polytechnic University, Hong Kong, China.

model-based method is powerful in dealing with abrupt changes. For example, Usoro et al. (1985) used this approach to detect an abrupt bias in a room temperature sensor. Henry and Clarke (1993) identified several disadvantages of the method: (1) it can be burdensome to develop models for different systems, (2) it is difficult to obtain dynamic models that are robust to plant modifications, and (3) the validity of the models used can be a problem. This latter problem applies to the highly nonlinear dynamic building HVAC systems. Therefore, Henry and Clarke (1993) proposed a SEVA (sensor-validating) approach as a solution. In a SEVA sensor, a built-in microprocessor examines the various signals within the sensor to detect and diagnose different faults (Yang and Clarke 1997; Clarke and Fraher 1996; Yung and Clarke 1989). This approach does not use system-level relationships among different variables that may be simple, easy to establish, and useful in certain situations.

The difficulty in distinguishing soft sensor faults from plant performance degradation or changes in working conditions is another problem with the model-based FDD method. Usually, both soft sensor faults and plant performance degradation occur naturally and simultaneously. It is difficult to separate them with a model-based method because the models used become invalid due to the presence of component faults.

Recently, Wang and Wang (1999) presented a conservation-law-based sensor fault detection, diagnosis, and evaluation (FDD&E) strategy. They developed several schemes to detect the existence, identify the location, and evaluate the magnitudes of sensor faults in the chilled water flow meters and temperature sensors in a typical chilling plant. The values of the sensor biases were estimated (Wang and Wang 1999, 2000). The strategy uses the relationships that are directly based on the universally valid steady-state mass and energy conservation laws. Such relationships are easy to set up and are not affected by the presence or the occurrence of most component faults, including equipment or system performance degradation or changes in plant working conditions. Only sensor faults can cause the apparent imbalances of mass or energy. Therefore, the law-based strategy not only avoids the model validity problem, but also can distinguish intrinsically sensor faults from component faults. Sensor biases are estimated by minimizing the sum of the squares of the associated balance residuals. The estimates successfully produced by the FDD&E schemes make it possible for building management systems (BMS) to automatically correct the faulty measurements.

This paper presents an integrated robust FDD&E strategy for the flow meters and temperature sensors in central chilling plants. The integrated strategy builds on the basic scheme described in Wang and Wang (1999) that improves the robustness of bias estimation in cooling water sensors. The robust scheme estimates the bias magnitudes of several chilled water sensors by minimizing systematically the sums of the squares of the associated energy balance residuals. A genetic algorithm is used to solve the corresponding multimodal minimization problem, which is difficult to solve by conventional gradient-directed searching methods. For the cooling water sensor FDD&E scheme, a correlation cancellation method is developed to estimate the cooling water flow meter bias.

The integrated robust strategy is validated using data generated by a dynamic simulation program for an existing chilling system. It is also applied to an existing building chilling system. The results of the simulation tests and the field application are presented and analyzed.

OVERVIEW OF INTEGRATED ROBUST STRATEGY

The system studied is a typical primary-secondary chilling plant commonly used in large building HVAC systems, as shown schematically in Figure 1. The sensors illustrated are necessary to facilitate different schemes of control, management, and condition monitoring in the plant. The building flow meter M_b and the supply and return temperature sensors (T_{sb}, T_{rb}) are necessary for measuring the building cooling load. The chilled water flow meter $M(j)$, the

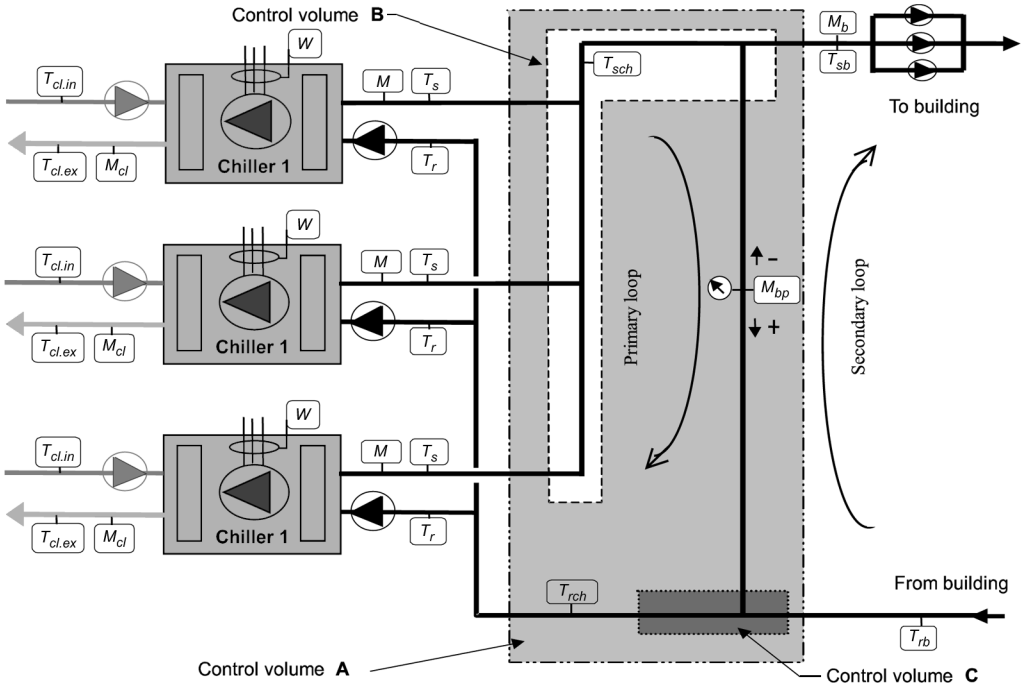

Figure 1. Schematic of Primary-Secondary Chilling System

supply and return temperature sensors $[T_s(j), T_r(j)]$, and the power meter $W(j)$ associated with each chiller are necessary for monitoring the evaporator water flow condition and assessing chiller performances. The cooling water flow meter $M_{cl}(j)$ and the temperature sensors at the inlet and outlet $[T_{cl.in}(j), T_{cl.ex}(j)]$ provide information about the condenser water flow condition and the performance of the associated heat rejection equipment, such as a cooling tower or an intermediate heat exchanger. The measurement from the bypass flow meter M_{bp} is an important reference for chiller sequencing control. In different situations, more or fewer sensors may be installed. For example, a temperature sensor in the return header T_{rch} may be used in addition to the individual return temperature sensors $T_r(j)$. Alternatively, a temperature sensor in the supply header T_{sch} may be available, or the cooling water flow meter $M_{cl}(j)$ may not be installed.

A flow switch is usually used in association with each chiller for detecting the corresponding chilled water flow on/off condition. $I(j)$ is used to denote this signal. When there is chilled water flowing through the evaporator, $I(j) = 1$; otherwise, $I(j) = 0$. A flow switch in the bypass line is used to indicate the flow direction, with I_{bp1} and I_{bp2} used to denote the direction signals. When the direction is positive, $I_{bp1} = 1$ and $I_{bp2} = 0$. When the flow direction is negative, $I_{bp1} = 0$ and $I_{bp2} = 1$. The bypass meter M_{bp} is regarded as two different meters. Field observations showed that the meter measurement signals in the two directions exhibit different characteristics. M_{bp1} and M_{bp2} are used to denote the positive and negative direction flows (meters), respectively.

The overall structure of the integrated robust FDD&E strategy is illustrated in Figure 2. The faults to be examined are the biases in the flow meters and temperature sensors described above. The sensor measurements and the relevant control signals are used as the input. The output is the estimate of the biases in the sensors. The strategy is composed of one scheme for the chilled water sensors and another one for cooling water sensor.

The robust FDD&E scheme consists of a basic (sequential) scheme and a robust [genetic algorithm (GA)] estimator. The sequential scheme is constructed by using several estimators

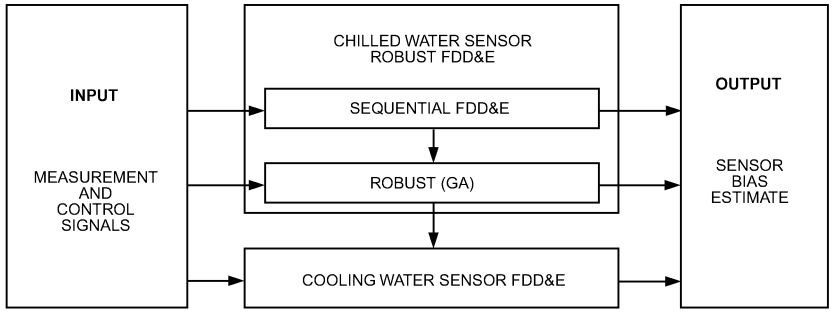

Figure 2. Integrated Sensor FDD&E Strategy

that are selected and configured according to given sensor installation conditions. The estimators in the sequential scheme estimate the biases in the chilled water flow meters and the temperature sensors. The GA estimator is used to improve the estimation accuracy. The strategy uses a temperature sensor with a bias that is either known or assumed to be zero as a common reference. The use of the common reference does not affect the estimation results of the associated flow meter biases, and the relative biases of the temperature sensors with each other are also not affected (Wang and Wang 1999).

The cooling water sensor scheme deals with the biases in the cooling water flow meters and the biases in the cooling water temperature sensors, using the chilled water sensor bias estimates as given parameters. If a cooling water flow meter is not installed, a constant flow rate is assumed and used as the measurement. In such a case, the estimates of the cooling water flow meter biases are the estimates of the guess errors.

METHODOLOGY

The sequential scheme consists of several estimators that minimize the balance residual square sum for individual control volumes and calculate the associated chilled water sensor biases sequentially. The method to establish the chilled water sensor bias estimators in a sequential FDD&E scheme and the definitions of the raw and corrected balance residuals for different control volumes are described in detail in Wang and Wang (1999). Eleven such estimators and an automatic method to select and configure these estimators have been developed for all possible sensor installation conditions in the plant (Wang 2000).

Two sequential schemes were used in the tests presented in this paper. One was that reported in Wang and Wang (1999) for the sensor installation condition, with the difference that, for $T_r(j)$ and T_{sch}, all of the chilled water sensors shown in Figure 1 were considered available. Four estimators (1, 2, 3, 4) were used. The return temperature sensor T_{rch} was used as the common reference.

The other scheme, illustrated by Figure 3, is for the sensor installation condition that all of the sensors shown in Figure 1 (except for the building return temperature sensor T_{rb}, those in the return header T_{rch}, and those in the supply header T_{sch}) are available. Due to the absence of the building return temperature sensor, Estimator 3 was not selected. An estimator (Estimator 8) was used to estimate the biases in the chiller return temperature sensors $\delta_{Tr}(j)$. Estimator 4 was revised to accommodate the situation when a building return temperature sensor is not installed. The control volume A (see Figure 1) heat balance residual is now calculated by Equation (1). Using $I_{bp2}^{[i]}$ means that $\hat{r}_A^{[i]}$ is calculated only for the measurements when the bypass flow is in the negative direction. $\hat{T}_{rch}^{[i]}$ is an artificial return temperature measurement calculated by Equation (2), which is used also as the common reference.

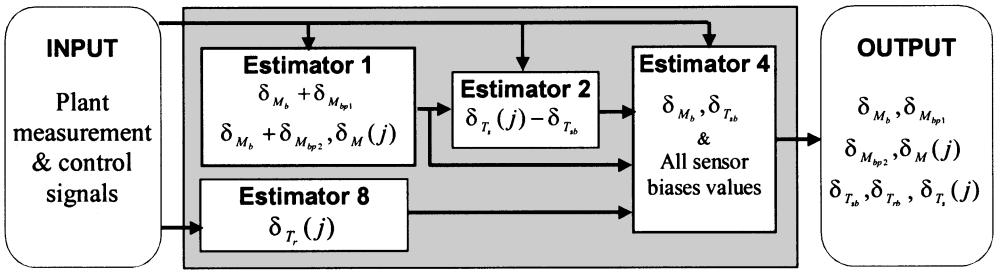

Figure 3. Sequential Scheme Estimators for Real Chilling Plant

$$\hat{r}_A^{[i]} = \rho c_{pw} I_{bp2}^{[i]} \{\hat{M}_b^{[i]}(\hat{T}_{rch}^{[i]} - \hat{T}_{sb}^{[i]}) - \sum_{j=1}^{N}[\hat{M}^{[i]}(j) I^{[i]}(j)(\hat{T}_{rch}^{[i]}(j) - \hat{T}_s^{[i]}(j)]\} \tag{1}$$

$$\hat{T}_{rch}^{[i]} = \frac{\sum_{j=1}^{N}(I^{[i]}(j)[\hat{T}_r^{[i]}(j) - \delta_{Tr}(j)])}{\sum_{j=1}^{N} I^{[i]}(j)} \tag{2}$$

Equation (3) represents the normal equation for Estimator 8, where $\mathbf{A}_8$ is an $N \times N$ square matrix and $\mathbf{b}_8$ is a vector. A detailed description of Estimator 8 is available in Wang (2000).

$$\mathbf{A}_8[\delta_{Tr}(1), \ldots, \delta_{Tr}(j), \ldots, \delta_{Tr}(N)]^T = \mathbf{b}_8 \tag{3}$$

Robust GA Estimator

The estimator is developed to increase the robustness using the previously described sequential schemes. The sequential schemes were found to perform well with dynamic simulation data in the condition when fixed sensor biases and random noises were introduced to the measurements. In practice, however, abrupt bias may occur to one or more of the associated sensors. A test, described later, showed that an abrupt bias with moderate magnitude and short duration in a temperature sensor would result in inaccurate estimates when a sequential FDD&E scheme was used alone. The main reason for the inaccuracy was that minimization of the balance residual square sum was applied to the heat balances for different control volumes individually and sequentially. Although the balance residual square sum for one control volume was minimized, the minimization of the residual square sums for other control volumes was sacrificed.

The robust estimator considers the associated heat balances systematically. It estimates the biases in the building flow meter and the building supply and chiller supply temperature sensors [δ_{Mb}, δ_{Tsb}, $\delta_{Ts}(j)$] by minimizing a new objective function [defined in Equation (4)], which is the sum of the mean squares of the normalized corrected heat balance residuals of control volume A and control volume B (see Figure 1). The number of the measurement samples used to analyze the steady-state heat balances for control volumes A and B are n_A and n_B, respectively. The minimization is

$$\text{minimize}|_{\delta_x}\left(\frac{\dot{S}_{rsq.A}}{n_A} + \frac{\dot{S}_{rsq.B}}{n_B}\right); \quad [\delta_x = \delta_{M_b}, \delta_{T_{sb}}, \delta_{T_s}(j), j = 1, \ldots, N \tag{4}$$

where

$$S_{rsq.A} = \sum_i (\dot{r}_A^{[i]})^2 \tag{5}$$

$$S_{rsq.B} = \sum_i (\dot{r}_B^{[i]})^2 \tag{6}$$

The normalized corrected residuals ($\dot{r}_A^{[i]}$, $\dot{r}_B^{[i]}$) are represented by Equations (7) and (8). The total number of the chillers that are operating at time [i] is $N_{op}^{[i]}$. If the chillers have different cooling capacities, the equivalent number of larger chillers is defined as the ratio of the nominal capacity to that of the smallest chiller.

$$\dot{r}_A^{[i]} = \frac{r_A^{[i]}}{N_{op}^{[i]}} = \frac{\hat{r}_A^{[i]}}{N_{op}^{[i]}} - \frac{\delta r_A^{[i]}}{N_{op}^{[i]}} \tag{7}$$

$$\dot{r}_B^{[i]} = \frac{r_B^{[i]}}{N_{op}^{[i]}} = \frac{\hat{r}_B^{[i]}}{N_{op}^{[i]}} - \frac{\delta r_B^{[i]}}{N_{op}^{[i]}} \tag{8}$$

In concept, Equation (4) could be reduced to solving the corresponding normal equations in the sensor biases, as was done in developing the estimators of the sequential FDD&E schemes. However, the resulting normal equations would be a system of polynomial equations that has $N + 2$ unknowns with the highest order of three. Such a set is difficult to solve using traditional gradient-directed search methods because multiple (local) minima and (local) maxima exist. As an alternative, a GA estimator is used, which is an advanced automatic search and optimization method. It is considered robust for finding the global maximum (Goldberg 1989). Equation (9) represents the fitness function.

$$f = f[\delta_M, \delta_{MT_{sb}}, \delta_{T_s}(j)] = \frac{1}{\frac{S_{rsq.A}}{n_A} + \frac{S_{rsq.B}}{n_B}} \tag{9}$$

Figure 4 shows the flow chart of the robust GA estimator. It starts with the bias estimates and steady-state measurement data obtained by the sequential FDD&E scheme. The component with grayed background represents the operation procedures in a GA run. The variables constituting the GA search space are the relative biases in the chiller supply temperature sensors with respect to the building supply temperature sensor [$\delta_{Ts}(j) - \delta_{Tsb}$]. The remaining two estimates (δ_{Mb} and δ_{Tsb}), corresponding to each of the GA trial sets, are determined internally by Estimator 4.

Two types of initialization are necessary at the beginning of each run in the GA estimator. One is a procedure within a GA that produces the initial population to start a GA run. The other is the initialization to set or reset the intervals of the search variables and the seed of the random number generator. For different runs, the seed is changed. The search interval is reset by using the initial estimate of each variable [$\delta_{Ts}(j) - \delta_{Tsb}$] as the center. A default radius is used to define the upper and lower limits.

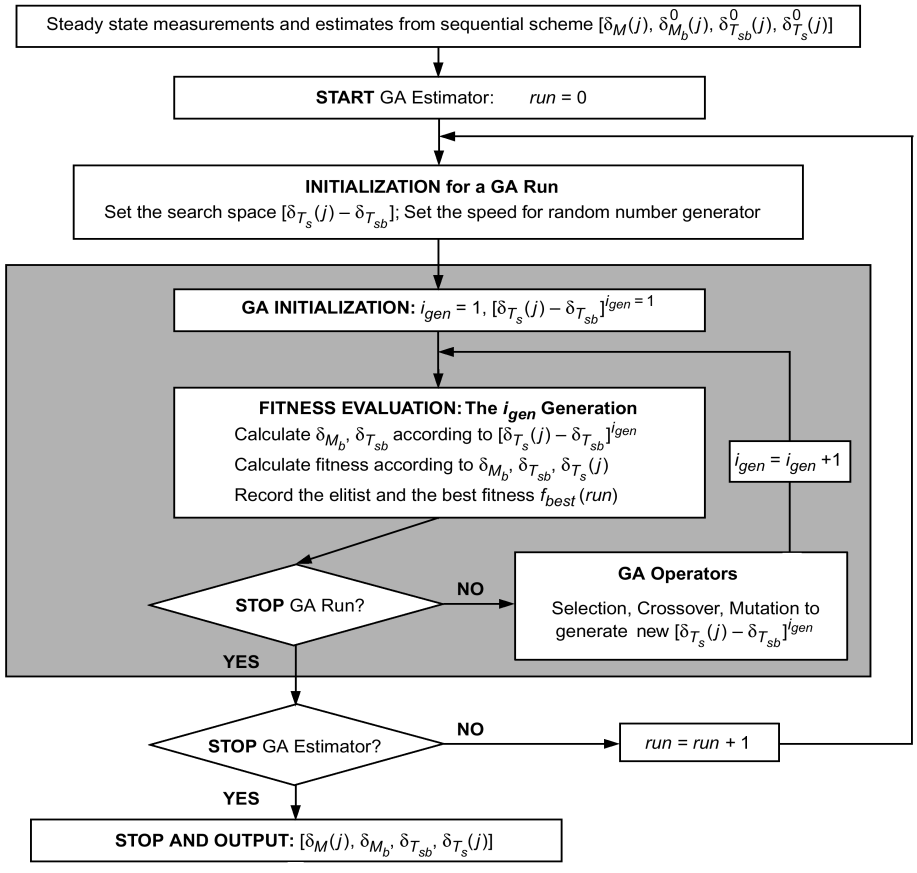

Figure 4. Flow Chart of GA Estimator

A GA run is terminated if the number of the current generation is equal to a prespecified maximum generation number. At least two runs of the GA processes are necessary when running the GA estimator. The criterion to stop the GA estimator is based on the comparison of the best fitness values of two consecutive runs. If the relative difference between the best fitness values of two consecutive GA runs is less than a given threshold value (e.g., 0.001), then the GA estimator is finished.

A Fortran GA driver developed by Carroll (1999) was used, with some adaptation to the source codes for implementing multiple runs and termination rules, and for resetting the control parameters. Detailed descriptions of the relevant issues can be found in Wang and Wang (2000).

FDD&E OF COOLING WATER SENSORS

An estimator is developed to estimate the bias in the cooling water flow meter and the relative bias in the exit temperature sensor with respect to the inlet temperature sensor [$\delta_{Mcl}(j)$, $\delta_{Tcl.ex}(j) - \delta_{Tcl.in}(j)$], given the biases in the associated chilled water sensors. The estimator is based on the energy balance for a chiller in steady-state operation.

A characteristic quantity is obtained from analyzing the energy balance residual. The characteristic quantity is able to indicate the existence of the chilled and cooling water flow meter biases, even when the biases in the temperature sensors and the chiller power meter are unknown. A correlation cancellation method is consequently developed to estimate the cooling

water flow meter bias. The relative cooling water temperature sensor bias is estimated by minimizing the corrected chiller energy balance residual square sum.

Equation (10) represents the chiller energy balance in steady state, where the index identifying a particular chiller (j) is omitted for brevity. The term Q denotes the rate of the overall chiller heat loss to the plant environment, which is considered approximately constant. The raw residual is defined as represented by Equation (11). The corrected chiller energy balance residual can be derived as represented by Equation (12).

$$W^{[i]} + \rho_{ch} c_{pch} M^{[i]} (T_r^{[i]} - T_s^{[i]}) - \rho_{cl} c_{pcl} M_{cl}^{[i]} (T_{cl.ex}^{[i]} - T_{cl.in}^{[i]}) - Q = 0 \tag{10}$$

$$\hat{r}_{ch}^{[i]} = \hat{W}^{[i]} - \rho_{ch} c_{pch} \hat{M}^{[i]} (\hat{T}_r^{[i]} - \hat{T}_s^{[i]}) - \rho_{cl} c_{pcl} \hat{M}_{cl}^{[i]} (\hat{T}_{cl.ex}^{[i]} - \hat{T}_{cl.in}^{[i]}) \tag{11}$$

$$\begin{aligned} r_{ch}^{[i]} = {} & Q + \nu_W^{[i]} + \rho_{ch} c_{pch} [M^i (\nu_{T_r}^{[i]} - \nu_{T_s}^{[i]}) + \Delta T_{ch}^{[i]} \nu_M^{[i]} + \nu_M^{[i]} (\nu_{T_r}^{[i]} - \nu_{T_s}^{[i]})] \\ & - \rho_{cl} c_{pcl} [M_{cl}^{[i]} (\nu_{T_{cl.ex}}^{[i]} - \nu_{T_{rcl.in}}^{[i]}) + \Delta T_{cl}^{[i]} \nu_{M_{cl}}^{[i]} + \rho \nu_{M_{cl}}^{[i]} (\nu_{T_{cl.ex}}^{[i]} - \nu_{T_{cl.in}}^{[i]})] \end{aligned} \tag{12}$$

where

$$\Delta T_{ch}^{[i]} = T_r^{[i]} - T_s^{[i]}$$

$$\Delta T_{cl}^{[i]} = T_{cl.ex}^{[i]} - T_{cl.in}^{[i]}$$

It can be shown that the statistical expectation $E(\hat{r}_{ch}^{[i]})$ of the corrected residual is constant and equals Q. When biases are present in the measurements the statistical expectation of the raw residual varies with the chiller working condition because $\Delta T_{ch}^{[i]}$ and $\Delta T_{cl}^{[i]}$ vary as the cooling load changes [see Equation (13)]. The power meter bias δ_W is assumed constant. The chilled and cooling water flow rates are also considered constant.

$$\begin{aligned} E(\hat{r}_{ch}^{[i]}) = {} & Q + \delta_W + c_{pch} [(M^{[i]} + \delta_M)(\delta_{T_r} - \delta_{T_s}) + \delta_M (\Delta T_{ch}^{[i]} + \delta_{T_r} - \delta_{T_s}) - \delta_M (\delta_{T_r} - \delta_{T_s})] \\ & - c_{pcl} \rho_{cl} [(M_{cl} + \delta_{M_{cl}})(\delta_{T_{cl.ex}} - \delta_{T_{cl.in}}) + \delta_{M_{cl}} (\Delta T_{cl}^{[i]} + \delta_{T_{cl.ex}} - \delta_{T_{cl.in}})] \\ & - \delta_{M_{cl}} (\delta_{T_{cl.ex}} - \delta_{T_{cl.in}}) \end{aligned} \tag{13}$$

Based on Equation (13), an approximate linear relationship [given by Equation (14)] can be found that correlates the raw chiller energy balance residuals to the chiller power inputs (Wang 2000). The slope α is a function of the chilled and cooling water flow meter biases (δ_M, δ_{Mcl}), the average coefficient of chiller performance $\overline{COP}$, and the true values of the chilled and cooling water flows (M and M_{cl}), as represented by Equation (15). The constant β is a function of the chiller heat loss Q, bias in the power meter δ_W, biases in the flow meters (δ_M, δ_{Mcl}), and the relative biases in the chilled and cooling water temperature sensors ($\delta_{\Delta Tch} = \delta_{Tr} \delta_{Ts}$, $\delta_{\Delta Tcl} = \delta_{Tcl.ex} \delta_{Tcl.in}$) [Equation (16)].

$$\hat{r}_{ch} = \alpha \hat{W} + \beta \tag{14}$$

$$\alpha = \frac{\delta_M \overline{COP}}{M} - \frac{\delta_{M_{cl}} (1 + \overline{COP})}{M_{cl}} \tag{15}$$

$$\beta = Q + (1 - \alpha) \delta_W + \rho_{ch} c_{pch} (M \delta_{\Delta T_{ch}} + \delta_M \delta_{\Delta T_{ch}}) - \rho_{cl} c_{pcl} (M_{cl} \delta_{\Delta T_{cl}} + \delta_{M_{cl}} \delta_{\Delta T_{cl}}) \tag{16}$$

The slope α is the characteristic quantity used to diagnose whether the flow meters are biased. As can be seen from Equation (15), if the flow meters are correct, the value of the slope is zero. If they are biased ($\delta_M \neq 0$, $\delta_{Mcl} \neq 0$), the slope is nonzero. This conclusion will not be affected by the value of the chiller heat loss, and any power meter bias or temperature sensor biases. The only exception is the situation represented by Equation (17), which can be regarded as an exceptional case:

$$\frac{\delta_M \overline{\mathrm{COP}}}{M} = \frac{\delta_{M_{cl}}(1 + \overline{\mathrm{COP}})}{M_{cl}} \tag{17}$$

The characteristic quantity α can be regressed against other variables from a set of measurement data using a standard linear regression method, as represented by Equation (18), where n is the sample size. Existence of the flow meter bias(es) can be detected if the absolute value of the characteristic quantity exceeds a tuned threshold value.

$$\alpha = \frac{\sum_i \hat{r}_{ch}^i \hat{W}^i - \frac{\sum_i \hat{W}^i \sum_i \hat{r}_{ch}^i}{n}}{\sum_i (\hat{W}^i)^2 - \frac{\sum_i (\hat{W}^i)^2}{n}} \tag{18}$$

Equation (19) is used to estimate the cooling water flow meter bias δ_{Mcl} when the chilled water flow meter bias δ_M is known. The estimation can be carried out independent of whether the biases in the chilled and the cooling water temperature sensors exist. If biases in the chilled and cooling water flow meters are removed from the measurement data, the correlation of the chiller energy balance residual to the chiller power input (Equation 14) would be cancelled. As a result, the corresponding slope becomes zero. Equation (19) is obtained by substituting the partially corrected chiller energy balance residuals obtained by correcting only the flow measurements into Equation (18), and by setting the denominator zero.

Equation (20) is used to estimate the relative cooling water temperature sensor bias when the relative chilled water temperature sensor bias is known. It is derived from minimizing the sum of squares of the fully corrected chiller energy balance residuals, obtained by correcting both the flow and temperature measurements, by assuming that the chiller heat loss and power meter bias are negligible ($Q \approx 0$, $\delta_W \approx 0$).

$$\delta_{M_{cl}} = -\frac{\left[\left(S_{r_{ch}W} - \frac{S_W S_{r_{ch}}}{n}\right) - \rho_{ch} c_{pch}\left(S_{\Delta T_{ch}W} - \frac{S_W S_{\Delta T_{ch}}}{n}\right)\delta_{ch}\right]}{\left[\rho_{cl} c_{pcl}\left(S_{\Delta T_{cl}W} - \frac{S_W S_{\Delta T_{cl}}}{n}\right)\right]} \tag{19}$$

$$\delta_{T_{cl.ex}} - \delta_{T_{cl.in}} = \frac{\frac{\rho_{ch} c_{pch}}{\rho_{cl} c_{pcl}}[(S_M - n\delta_M)(\delta_{T_r} - \delta_{T_s}) + S_{\Delta T_{ch}}\delta M] - \frac{S_{rch}}{\rho_{cl} c_{pcl}} - S_{\Delta T_{cl}}\delta_{M_{cl}}}{S_{M_{cl}} - n\delta_{M_{cl}}} \tag{20}$$

Further descriptions of the two estimation equations are given in Wang (2000). The formulas calculating the summations S in the above two equations are given in the Appendix.

SIMULATION RESULTS

The strategy was validated through various tests using dynamic simulation data. Two tests are presented below. In Test 1, the robust FDD&E scheme for the chilled water sensors was validated and compared with the sequential scheme in an unfavorable condition. Both the sequential and robust schemes performed satisfactorily under normal conditions.

Test 2 is for validating the cooling water sensor biases estimation method. A TRNSYS (Klein 1994) program developed to simulate an existing chilling system (Wang 1998) simulated four identical-duty chillers. The sensors considered available were those that were specified for the first sequential scheme described in Section 3. Fixed sensor biases were introduced throughout the simulation. Random noises were added to sensor outputs at each simulation step.

For Test 1, measurements from four days (96 hours) of operation were used. The biases introduced into the chilled water sensors are given in Table 1. In addition to the fixed sensor biases and random noises, an abrupt bias with a small magnitude (0.3°C) and short duration (approximately 40 min) was introduced into the building supply temperature sensor (T_{sb}). No bias was introduced into the common reference temperature sensor (T_{rch}).

The results from both the sequential and robust FDD&E schemes are also listed in Table 1. As can be seen in the estimates from the sequential scheme, the abrupt bias in the building supply temperature sensor noticeably affected not only the temperature sensor bias estimate, but also that of the chiller supply temperature sensors and the building and bypass flow meters. The largest error of the temperature sensor bias estimates was about 0.54°C [$\delta_{Ts}(3)$]. Such an error would probably not be tolerated in the chilled water sensors because the differential temperatures are usually small (e.g., 4 to 6°C). On the other hand, the result from the robust scheme was much better. The building flow meter bias estimate by the robust scheme was closer to the introduced value than that by the sequential scheme. The estimate of the building supply temperature sensor bias was –0.763°C, which was much closer to the true value (–0.651°C) compared to the sequential scheme estimate of –0.994°C. The largest error of temperature sensor bias estimates was reduced from 0.54 to 0.16°C [$\delta_{Ts}(3)$]. The bias estimates of the individual chiller flow meters [$M(1)$ to $M(4)$] by the two schemes are the same.

Table 1. Test Condition and Results: Test 1

	Introduced Bias			Estimates	
Sensor	Fixed	Abrupt (Duration)	Time Average	Robust Scheme	Sequential Scheme
M_b	–14.04	—	–14.04	–11.818	–7.035
T_{sb}	–0.653	0.3 (19.06 to 19.46)	–0.651	–0.763	–0.944
T_{rb}	0.414		0.414	0.410	0.410
M_{bp1}	–1.535	—	–1.535	–2.625	–5.407
M_{bp2}	5.721	—	5.721	3.099	0.317
$M(1)$	12.24	—	12.24	11.96	11.96
$M(2)$	2.28	—	2.28	2.19	2.19
$M(3)$	–13.82	—	–13.82	–13.87	–13.87
$M(4)$	–2.17	—	–2.17	–2.17	–2.17
$T_s(1)$	1.582	—	1.582	1.450	1.077
$T_s(2)$	–0.034	—	–0.034	–0.092	0.124
$T_s(3)$	–0.099	—	–0.099	–0.257	–0.630
$T_s(4)$	0.650	—	0.650	0.497	0.130

Units: Flow, L/s; Temperature, °C

Table 2. Test Condition and Results: Test 2

Chiller No.	1	2	3	4
Cooling water flow rate M_{cl} (L/s)				
Introduced	100	153	133	133
Estimated	98.8	153.8	132.0	134.5
Temperature sensor ($T_{cl.ex} - T_{cl.in}$) bias (°C)				
Introduced	–0.57	1.32	1.62	–1.10
Estimated	–0.56	1.31	1.70	–1.14
Power meter bias W (kW), introduced	1.9	61.2	42.3	75.1

An abrupt bias in the temperature sensor of a small magnitude and short duration resulted in noticeable inaccuracy in the bias estimations of the building and bypass flow meter biases and in all the chilled water temperature sensors when using the sequential scheme. The introduced abrupt bias happened to be in a period that corresponds to one combination of chillers in use. The misleading information in the period affected the output of Estimator 2, the relative biases of the individual chiller supply temperature sensor with respect to the building supply temperature sensor [$\delta_{Ts}(i) - \delta_{Tsb}$], which further influenced the output of Estimator 4. Wang and Wang (1999) demonstrate the solution sequence of the scheme.

When using the sequential scheme, the heat balance residual square sum for the control volume B was indeed minimized, but not that for the control volume A. Although the latter might be considered to have been minimized if the bias in the building flow meter and the building supply temperature sensor were considered to be the only variables affecting the balances, it was not globally minimized since it was also affected by the biases in the chiller supply temperature sensors $T_s(j)$. The chiller supply temperature sensor biases could be adjusted further to minimize control volume A's heat balance residual square sum, and the control volume B heat balance residual square sum was not significantly affected. The minimization object function of the GA estimator has considered these two heat balances globally, and, consequently, improved the accuracy of the sensor bias estimates.

In Test 2, the chilled water sensors considered available were those specified for the second sequential scheme mentioned in Section 3 (see Figure 3). The cooling water inlet and outlet temperature sensors were available, but the cooling water flow meters M_{cl} were not. The biases introduced into the cooling water temperature sensors and the cooling water flow rate associated with each chiller and the corresponding estimates are shown in Table 2. The chilled water sensors are not given because this test focused on the cooling water sensors. The temperature sensor biases are given by their relative values. The design cooling water flow rates (133 L/s) were used as the measurements. Obstructions in the cooling water circuit of chiller 1 and increased cooling water flow of chiller 2 were simulated. Biases were introduced into chiller power meters W.

The estimates and the corresponding true values are compared in Table 2. The estimation results were very good. The estimates of the relative cooling water temperature sensor biases were obtained by assuming that the power meter biases and the chiller heat losses were zero. The effects of the power meter biases on the estimates of the relative temperature sensor biases were not significant, although three of the power meter biases were actually quite large.

FIELD TESTS

The integrated robust strategy was tested in the chilling plant an office building with 46 stories and a usable area of about 74 000 m^2. Figure 5 shows the schematic of the chilling plant. The system operates 24 h/day with five identical centrifugal chillers installed, four for duty and one for standby. Each chiller has a design cooling capacity of 3100 kW. An indirect seawater cooling system is used for heat rejection. A primary chilled water pump, a cooling water pump, and a

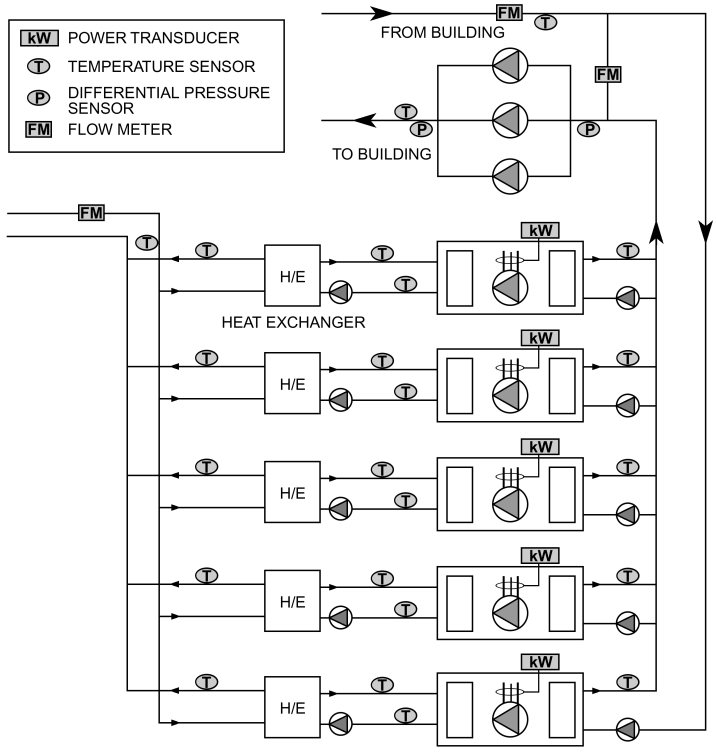

Figure 5. Existing Chilling System

seawater heat exchanger are associated with each chiller. Both the primary and secondary pumps are constant speed. The BMS sensors in the chilling plant include the building flow meter and supply temperate sensor (M_b, T_{sb}), the bypass flow meter M_{bp}, and the chilled water flow meter, supply and return temperature sensors, cooling water inlet, and outlet temperature sensors associated with each chiller [$M(j)$, $T_s(j)$, $T_r(j)$, $T_{cl.in}(j)$, $T_{cl.ex}(j)$]. Neither building return temperature sensors T_{rb} nor cooling water flow meters [$M_{cl}(j)$] for each chiller were installed. The sensors installed in the seawater network are not considered in this study.

Measurement data over several days were recorded in the BMS, and retrieved from the central computer station. The sampling interval was 5 min. Before the data were collected, the temperature sensors had been roughly calibrated on site. Biases were artificially introduced into three chilled water temperature sensors T_{sb}, $T_s(2)$, and $T_s(3)$ and one cooling water temperature sensor $T_{cl.in}(4)$ by changing the parameters of the relevant temperature sensors. The values of the introduced biases are given in Table 3.

Table 4 shows the results from applying the FDD&E strategy to the measured data. The bias estimates of the chilled water flow meter M and the estimates of the cooling water flow rates M_{cl} are absolute values. Individual chilled water temperature sensor bias estimates are relative with respect to the artificial common reference temperature T_{rch}. The cooling water temperature sensor biases are relative, the outlet with respect to the inlet [$\Delta T_{cl}(j) = T_{cl.ex}(j) - T_{cl.in}(j)$]. The bias estimates in the relative chilled water temperature sensors associated with each chiller [$\Delta T_{ch}(j) = T_r(j) - T_s(j)$], the return with respect to the supply, are also listed.

As shown in Table 4, the biases introduced into the chilled water temperature sensors T_{sb}, $T_s(2)$, and $T_s(3)$ were estimated successfully with good accuracy. For the remaining chilled water temperature sensors, the estimated biases were approximately zero. The effects of the

Table 3. Biases Manually Introduced into Three Temperature Sensors

Temperature sensor	T_{sb}	$T_s(2)$	$T_s(3)$	$T_{cl.in}(4)$
Introduced bias (°C)	1.5	1.0	–1.5	1.0

Table 4. Bias Estimates of Sensors in Existing Chilling Plant

Chilled Water Side						
Sensor	M_b	$M(1)$	$M(2)$	$M(3)$	$M(4)$	$M(5)$
Bias estimate	–4.9	3.2	17.9	17.7	6.8	17.0
Sensor	T_{sb}	$T_s(1)$	$T_s(2)$	$T_s(3)$	$T_s(4)$	$T_s(5)$
Bias estimate	1.75	–0.08	1.10	–1.47	0.14	0.27
Sensor	M_{bp1}	$T_r(1)$	$T_r(2)$	$T_r(3)$	$T_r(4)$	$T_r(5)$
Bias estimate	–2.2	–0.24	–0.11	0.04	0.24	0.08
Sensor	M_{bp2}	$\Delta T_{ch}(1)$	$\Delta T_{ch}(2)$	$\Delta T_{ch}(3)$	$\Delta T_{ch}(4)$	$\Delta T_{ch}(5)$
Bias estimate	16.8	–0.16	–1.21	1.51	0.10	–0.19
Cooling Water Side						
Flow rate		$M_{cl}(1)$	$M_{cl}(2)$	$M_{cl}(3)$	$M_{cl}(4)$	$M_{cl}(5)$
Flow rate estimate		142.1	138.9	134.7	137.6	145.3
Flow rate		$\Delta T_{cl}(1)$	$\Delta T_{cl}(2)$	$\Delta T_{cl}(3)$	$\Delta T_{cl}(4)$	$\Delta T_{cl}(5)$
Flow rate estimate		–0.23	–0.22	0.35	–1.28	–0.24

Units: Flow meter bias (flow rate), L/s; Temperature sensor bias, °C

biases in chiller 2 and 3 supply temperature sensors on the corresponding differential temperatures [$\Delta T_{ch}(2)$, $\Delta T_{ch}(3)$] were also correctly diagnosed. The relative bias in the cooling water temperature sensors of chiller 4 [$\Delta T_{cl}(4)$] resulting from the bias introduced into the inlet temperature sensor $T_{cl.in}(4)$ was estimated satisfactorily. For those differential temperatures (both chilled and cooling water) into which no bias had been introduced, the estimated relative biases were close to zero.

The flow meters associated with chillers 2, 3, and 5 [($M(2)$, $M(3)$, $M(5)$] and the bypass flow meter for the negative direction M_{bp2} were found to have large biases. The chilled water flow measurements for chillers 2, 3, and 5 were more than 10% larger than the true values. The cooling water flow rates of the five chillers were estimated to be 142.1, 138.9, 134.7, 137.6, and 145.3 L/s, respectively. The original commissioning record of the cooling water flow rates were 133 L/s. The relative estimation errors for chillers 2, 3, and 4 were below 5%, and for chillers 1 and 5 were within 10%.

DISCUSSION

The estimates of the biases in individual chilled water temperature sensors were not expected to be so accurate because the FDD&E strategy was developed to estimate them with respect to a common reference temperature sensor. The largest error in the chilled water temperature sensor biases was about 0.25°C (for T_{sb}). The accurate result was due to the use of the artificial return temperature T_{rch}. Using it as the common reference implied that the mean of the chiller return temperature sensor biases $\delta_{Tr}(j)$ would be zero. Because these temperature sensors had been calibrated before collecting the data, the real biases in the five return temperature sensors $T_r(j)$ could be regarded as randomly distributed around zero. In such a circumstance, the implicit assumption was, essentially, the real situation.

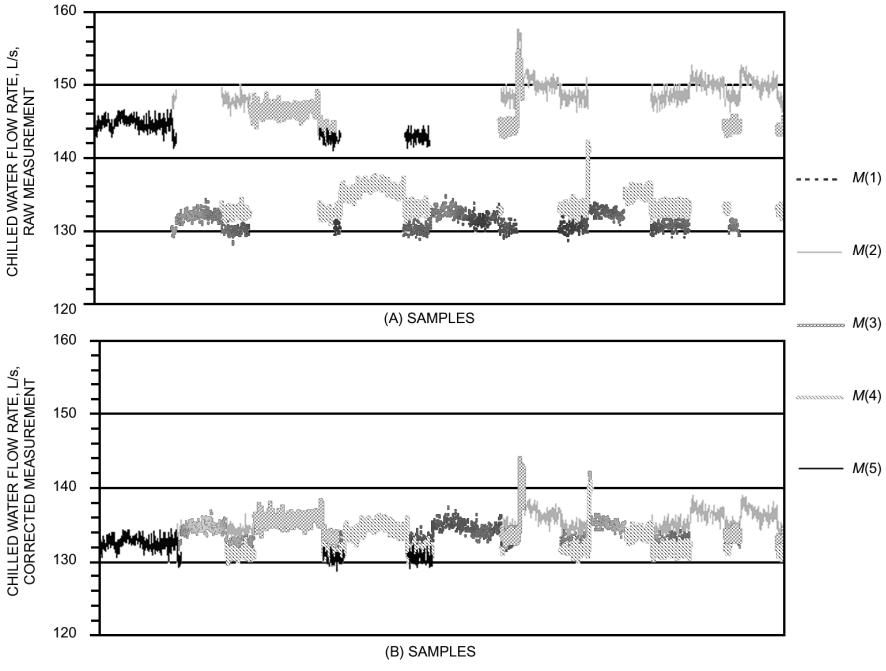

Figure 6. (A) Raw and (B) Corrected Chilled Water Flow Rates of Chillers (Site Test)

The corrected chilled water flow rates were examined for indirect verification of the flow meter bias estimates because there was no simple way to determine the true conditions directly. Figure 6 shows the raw and corrected chilled water flow rates of the five chillers. It can be seen in Figure 6A that the raw flow rates of different chillers were different from one another, even when they were operating at the same time. The largest difference was approximately 20 L/s. This finding seems to contradict the fact that the chillers and the primary pumps were identical and, thus, the flow rates of the chillers should have been approximately the same. However, as illustrated in Figure 6B, the corrected flow rates are close to each other, and near the commissioning record of 130 L/s.

Existence of the flow meter biases was more clearly indicated by the chilled water flow balance residuals. As shown in Figure 7, the raw balance residual exhibited obvious deviation from zero. In several periods, the imbalance of the water flow amounted to more than 40 L/s. The two possible reasons other than the meter faults that might lead to the deviations are serious leakage in the chilling plant and unmeasured bypass flows through the evaporators of idle chillers. However, no noticeable leakage was found on the site. By tracing both the supply and return temperatures of each chiller, it was found that bypass flow through the evaporators of idle chillers did not occur. Both temperatures rose normally after the chillers were shut down, and they approached the plant environment temperature after enough idle time. Therefore, the only factor that resulted in violation of the chilled water flow balance constraint was that bias(es) existed in some or all of the flow meters. After the biases had been eliminated, the corrected flow balance residuals became approximately random variables with zero mean, as can be seen in Figure 7.

The large bias of 1.5°C introduced into the building supply temperature sensor T_{sb} was clearly reflected in the heat balance residuals for the control volume A and B, as shown in Figures 8A and B, respectively. Both raw residuals deviate significantly from zero. After all the raw measurements had been corrected with the obtained bias estimates, the large deviations in the balance residuals were reduced.

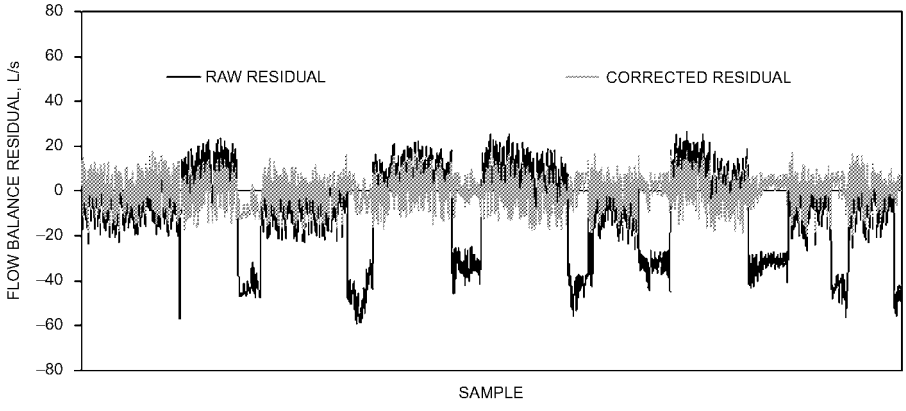

Figure 7. Chilled Water Flow Balance Residuals (Site Test)

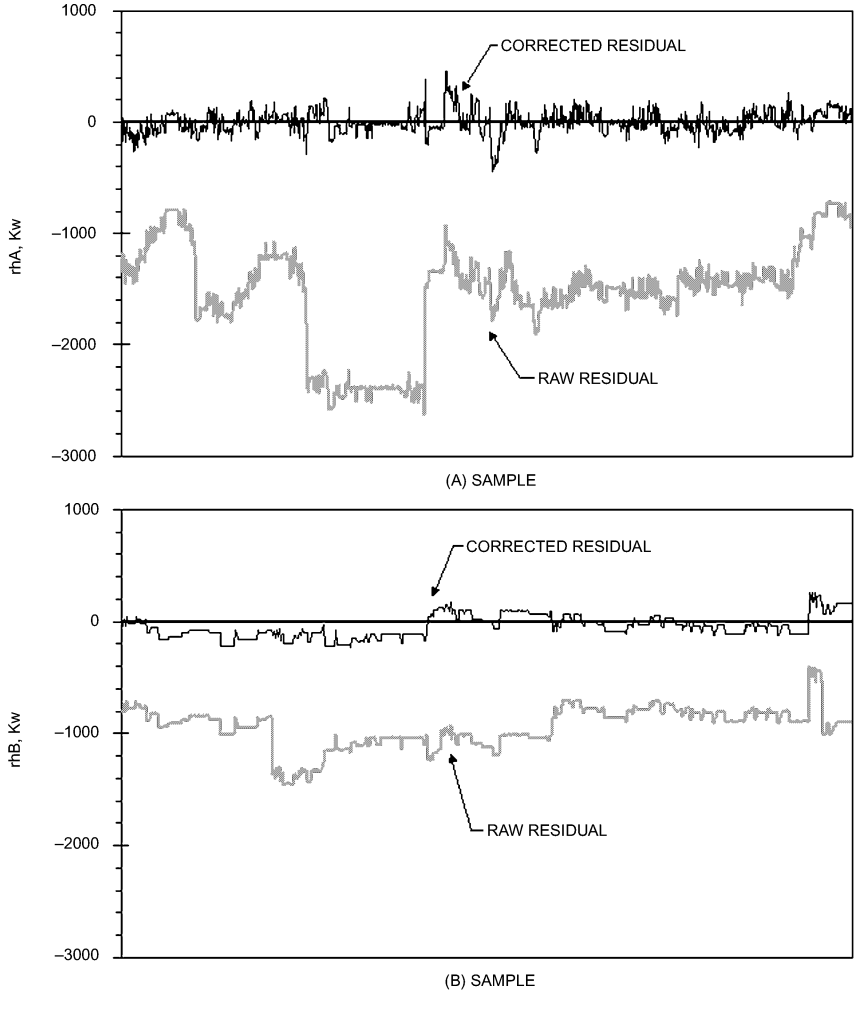

Figure 8. Heat Balance Residuals: (A) Control Volume A, and (B) Control Volume B (Site Test)

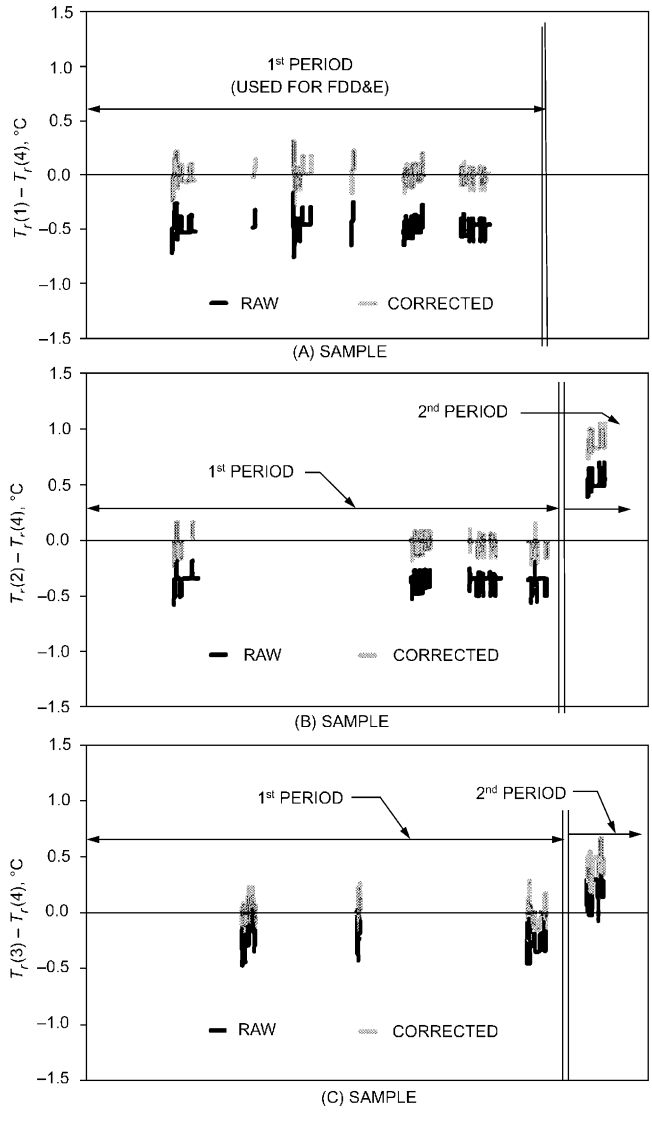

Figure 9. Chiller Return Temperature Sensor Redundancy Residuals (Site Test)

Figure 9 shows three redundancy residuals of the physically redundant chiller return temperature sensors [$T_r(1) - T_r(4)$, $T_r(2) - T_r(4)$, $T_r(3) - T_r(4)$]. The samples in the figure were from two different periods. The first period data were those that were used for the FDD&E test. The second short period data were collected about one month later to determine whether the temperature sensor biases changed. As can be seen in the figures, small biases in the sensors existed in the first period. The relative bias in the return temperature sensor of chiller 4 with respect to the return temperature sensor of chiller 1 was larger, about 0.5°C. The other two were smaller. The corrected residuals in the first period were around zero. Figures 9B and C show that the biases in the three temperature sensors $T_r(2)$, $T_r(3)$, and $T_r(4)$ changed between the first and second periods. Bursts of data points appear in this figure because any two chillers in the plant were not always operating simultaneously and measurement data were in a transient state.

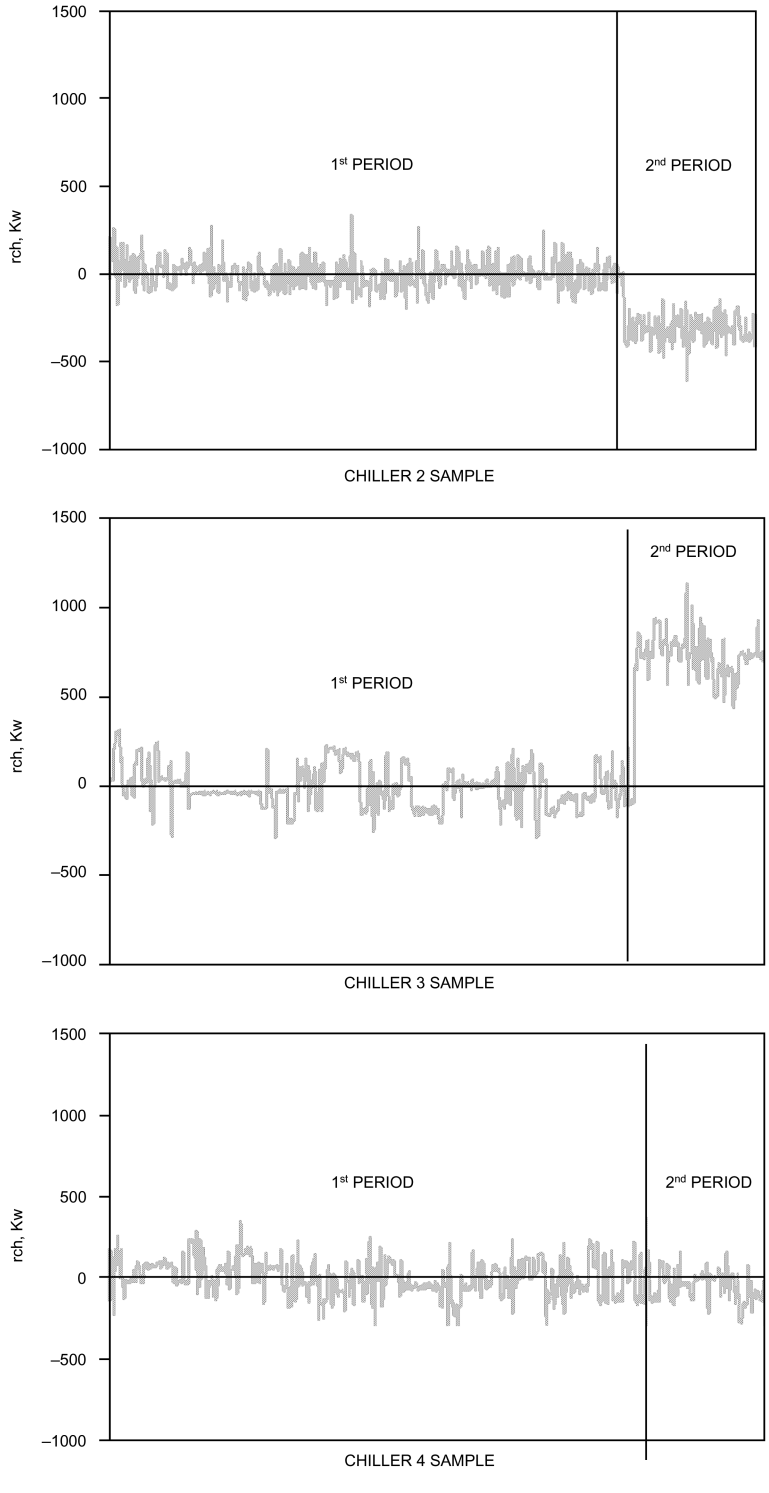

Figure 10. Corrected Energy Balance Residuals of Chillers (Site Test)

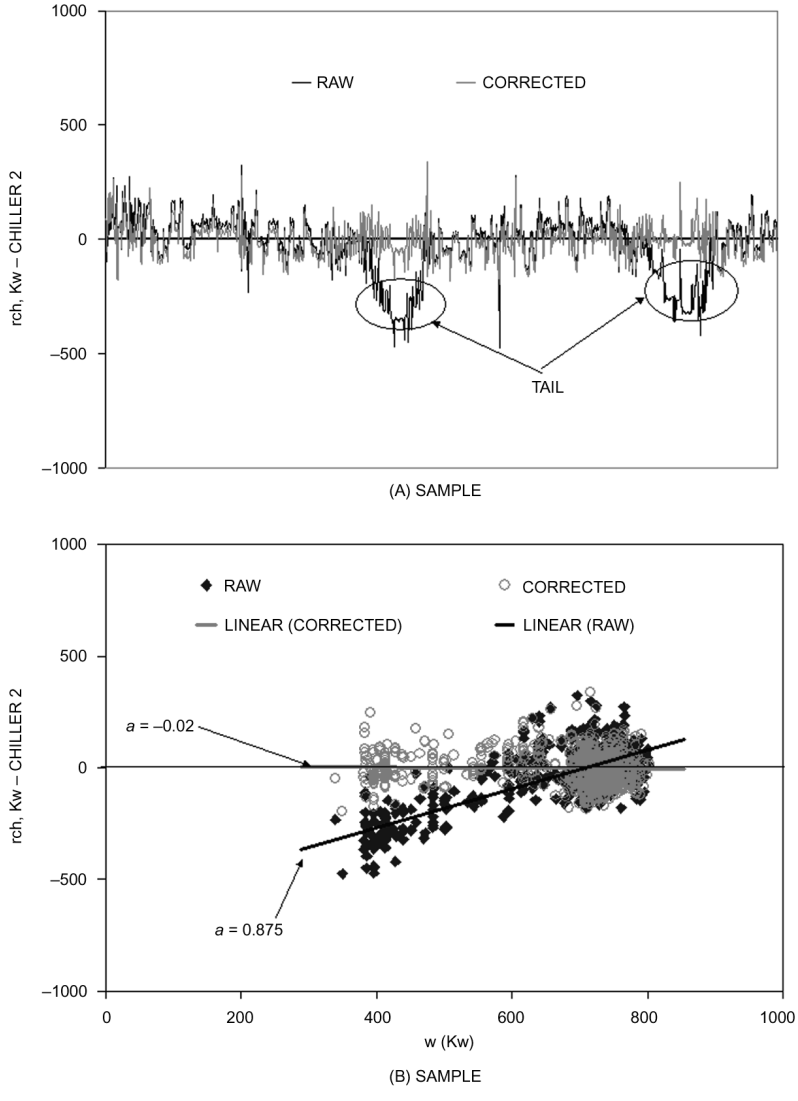

Figure 11. Chiller Energy Balance Residual: (A) Time Series, and (B) Drawn Against Power (Site Test)

The change in the biases in the chiller return temperature sensors was also reflected in the chiller energy balance residuals. Figure 10 shows the energy balance residuals of chillers 2, 3, and 4 that were corrected using the estimates obtained from the first period data. The corrected energy balance residuals for the three chillers in the first period were approximately random variables around zero, and that the mean of the residuals of chillers 2 and 3 in the second period deviated from zero while that of chiller 4 remained unchanged. By examining Figures 9 and 11, it can be concluded that the biases in the return temperature sensors for chillers 2 and 3 changed.

Figure 11 shows the energy balance residuals of chiller 2 as a time series and as a function of chiller power. The raw and the corrected residuals as a time series were very close to each other if the two tails in the raw residual were ignored. The time series of the raw residual alone did not clearly indicate either the introduced bias in the supply chilled water temperature sensor

[$\delta_{Ts}(2) = 1.0^{\circ}C$; see Table 3] or the existing bias in the chilled water flow meter [$\delta_M(2) = 17.9$ L/s; see Table 4] because the two faults compensated for each other. However, the existence of the chilled water flow meter fault could be clearly revealed by the characteristic quantity: the slope, which was large ($\alpha = 0.875$), regressed using the raw measurements.

CONCLUSION

A robust sensor FDD&E strategy for a typical chilling plant that integrates a robust chilled water sensor FDD&E scheme and a FDD&E scheme for the cooling water sensors was developed. Both the schemes are based on the fundamental physical conservation laws.

Biases in chilled water flow meters and temperature sensors were estimated by minimizing the sum of squares of the associated balance residuals. The robust chilled water sensor FDD&E scheme improved the performance of a pure sequential FDD&E scheme by considering globally the associated heat balances for different control volumes. A genetic algorithm, which is simple to implement and robust in obtaining global minimum solutions, was used as the minimization tool. A characteristic quantity was developed and used in the cooling water sensor FDD&E scheme for detection and estimation of chiller cooling water flow meter bias. The detection and estimation are robust with regard to unknown chiller heat loss, unknown chiller power meter bias, and unknown temperature sensor biases.

The integrated robust sensor FDD&E strategy performed very well in both simulation and field tests. Because the strategy is directly based on the flow and steady-state heat balances, it is able to accommodate equipment faults such as performance degradation and obstructions in pipelines.

ACKNOWLEDGEMENT

The work presented is financially supported by a grant (PolyU 5016/99E) from the Research Grants Council of the Hong Kong Special Administrative Region (SAR). The work is also the contribution of the authors in the Internal Energy Agency (IEA) research project, Annex 34 (Application of Fault Detection and Diagnosis in Real Buildings).

NOMENCLATURE

A	coefficient matrix
b	vector of constant
c_p	specific heat, kJ/(kg·K)
f	fitness value or fitness function; function
I	index denoting operation or direction status (0,1)
M	chilled water flow meter or the flow rate, L/s
N	total number of chillers in the plant
N_{op}	total number of chillers operating simultaneously
n	total number of sample points
r	residual
S	sum
T	temperature sensor or temperature, °C
W	power meter or power input, kW
α	slope
β	constant
δ	constant additive sensor bias

Superscripts

^	sample value
·	normalized variable
[i]	sampling instant
i_{gen}	number of generation
—	average value

Subscripts

A	related to control volume A
B	related to control volume B
C	related to control volume C
b	related to building
bp	related to bypass flow
$bp1$	related to bypass flow in positive direction
$bp2$	related to bypass flow in negative direction
ch	chilled water or chiller
cl	cooling water
ex	outlet
in	inlet
r	return
s	supply
sq	square

REFERENCES

Carroll, D.L. 1999. *FORTRAN Genetic Algorithm (GA) Driver*. Version 1.7.0. http://www.staff.uniuc.edu/~carroll/ga.html.

Clarke D.W. and P.M.A. Fraher. 1996. Model-Based Validation of a DOx Sensor. *Control Engineering Practice* 4(9):1313-1320.

Dexter, A.L. 1999. Control and Fault Detection in Buildings. *The 3rd International Symposium on Heating, Ventilating and Air Conditioning,* pp. 39-50. Shenzhen, China.

Goldberg, D.E. 1989. *Genetic Algorithms in Search, Optimization, and Machine Learning*. New York: Addison-Wesley.

Henry, M.P. and D.W. Clarke. 1993. The Self-Validating Sensor: Rationale, Definitions and Examples. *Control Engineering Practice* 1(4):585-610.

Kao, J.Y. and E.T. Pierce. 1983. Sensor Errors: Their Effects on Building Energy Consumption. *ASHRAE Journal* 42-45.

Klein, S. 1994. TRNSYS Version 14.1.

Lee, W.Y., J.M. House, and D.R. Shin. 1997. Fault Diagnosis and Temperature Sensor Recovery for an Air-Handling Unit. *ASHRAE Transactions* 103(1):621-633.

Patton, R.J. 1994. Robust Model-Based Fault Diagnosis: The State of The Art. *IFAC Symposium*, *Fault Detection, Supervision and Safety for Technical Process*, pp. 1-24. Espoo, Finland.

Phelan, J., M. Brandemuehl, and M. Krarti. 1996. Review of Laboratory and Field Methods to Measure Fan, Pump, and Chiller Performance. *ASHRAE Transactions* 103(2):914-925.

Pike, P. and K. Pennycook. 1992. *Commissioning of BEMS—A Code of Practice.* AH 2/92. BSRIA.

Stylianou, M. and D. Nikanour. 1996. Performance Monitoring, Fault Detection, and Diagnosis of Reciprocating Chillers. *ASHRAE Transactions* 102(1):615-627.

Usoro, P.B., L.C. Schick, and S. Negahdaripour. 1985. An Innovation-Based Methodology for HVAC System Fault Detection. *Journal of Dynamics Systems, Measurement, and Control. Transactions of the ASME* 107:284-285.

Wang, J.B. 2000. *Sensor Fault Diagnosis and Validation of Building Air Conditioning Systems*. Ph.D. dissertation, Hong Kong Polytechnic University.

Wang, S.W. 1998. Dynamic Simulation of A Building Central Chilling System and Evaluation of EMCS On-Line Control Strategies. *Building and Environment* 33(1):1-20.

Wang S.W. and J.B. Wang. 1999. Law-Based Sensor Fault Diagnosis and Validation for Building Air-conditioning Systems. *International Journal of HVAC&R Research* 5(4):353-380.

Wang, S.W. and J.B. Wang. 2000. Robust Sensor Fault Diagnosis and Validation in HVAC Systems. *Transactions of the Institute of Measurement and Control.*

Yang, J.C.Y. and D.W. Clarke. 1997. A Self-Validating Thermocouple. *IEEE Transactions on Control Systems Technology* 5(2):239-253.

Yung, S.K., and D.W. Clarke. 1989. Local Sensor Validation. *Measurement and Control* 22:132-150.

APPENDIX: SUMMATIONS IN EQUATIONS (19) AND (20)

$$S_{r_{ch}W} = \sum_i (\hat{r}_{ch}^{[i]} \hat{W}^{[i]}) \qquad S_{r_{ch}} = \sum_i \hat{r}_{ch}^{[i]} \qquad S_W = \sum_i \hat{W}^{[i]} \qquad S_{W^2} = \sum_i (\hat{W}^{[i]})^2$$

$$S_{\Delta T_{cl}W} = \sum_i (\Delta \hat{T}_{cl}^{[i]} \hat{W}^{[i]}) \quad S_{\Delta T_{cl}} = \sum_i \Delta \hat{T}_{cl}^{[i]} \quad S_{\Delta T_{ch}W} = \sum_i (\Delta \hat{T}_{ch}^{[i]} \hat{W}^{[i]}) \quad S_{\Delta T_{ch}} = \sum_i \Delta \hat{T}_{ch}^{[i]}$$

$$S_M = \sum_i \hat{M}^{[i]} \qquad S_{M_{cl}} = \sum_i \hat{M}_{cl}^{[i]}$$